Unusual Nuclear Structures in Meiotic Prophase of Fission Yeast: a Cytological Analysis

Jürg Bähler,* Toni Wyler,‡ Josef Loidl,§ and Jürg Kohli*

*Institute of General Microbiology, University of Bern, CH-3012 Bern, Switzerland; ‡Institute of Zoology, University of Bern, Switzerland; and §Department of Cytology and Genetics, Institute of Botany, University of Vienna, Austria

Abstract. Earlier results from sectioned nuclei indicating that *Schizosaccharomyces pombe* does not develop a classical tripartite synaptonemal complex (SC) during meiotic prophase are confirmed by spreading of whole nuclei. The linear elements appearing during prophase I resemble the axial cores (SC precursors) of other organisms. The number of linear elements in haploid, diploid, and tetraploid strains is always higher than the chromosome number, implying that they are not formed continuously along the chromosomes. Time course experiments reveal that the elements appear after DNA replication and form networks and bundles. Later they separate and ∿24 individual elements with a total length of 34 μm are observed before degradation and meiotic divisions. Parallel staining of DNA reveals changes in nuclear shape during meiotic prophase. Strains with a *mei4* mutation are blocked at a late prophase stage. In serial sections we additionally observed a constant arrangement of the spindle pole body, the nucleolus, and the presumptive centromere cluster.

Thus, *S. pombe* manages to recombine and segregate its chromosomes without SC. This might correlate with the absence of crossover interference. We propose a mechanism for chromosome pairing with initial recognition of the homologs at the centromeres and suggest functions of the linear elements in preparation of the chromosomes for meiosis I disjunction. With the spreading technique combined genetic, molecular, and cytological approaches become feasible in *S. pombe*. This provides an opportunity to study essential meiotic functions in the absence of SCs which may help to clarify the significance of the SC and its components for meiotic chromosome structure and function.

DURING meiosis, DNA replication is followed by two rounds of nuclear divisions resulting in haploid gametes that are required for sexual reproduction of eukaryotes. The first meiotic division (reductional division) is preceded by a complex series of events that result in pairing of the homologous chromosomes and high levels of genetic recombination. These meiosis-specific events occur during prophase I and are required for segregation of the homologous chromosomes during the reductional division. After premeiotic DNA replication, proteinaceous filaments, called axial cores, form along each chromosome and connect the sister chromatids. The process of chromosome pairing culminates in the formation of a continuous synaptonemal complex (SC)[1] between the homologous chromosomes (for review, see Giroux, 1988). The SC is a tripartite structure consisting of two axial elements (or lateral elements) which are closely synapsed at a distance of ∿100 nm and a central component which extends longitudinally between the two axial elements. The structure of the SC is highly conserved in the great majority of eukaryotes. It is assumed to be involved in meiotic recombination, homologous chromosome pairing, and segregation (for review, see von Wettstein et al., 1984). Although the SC was discovered more than 30 yr ago (reviewed by Moses, 1968), its particular functions are still unknown. Likewise, the processes of homologous chromosome recognition and pairing, as well as the role that meiotic recombination plays therein, are poorly understood (for reviews, see Giroux, 1988; Loidl, 1990; Roeder, 1990; Kleckner et al., 1991).

The fission yeast *Schizosaccharomyces pombe* normally enters meiosis immediately after fusion of two haploid cells of different mating type (zygotic meiosis), but diploid cells can also be induced to enter an azygotic meiosis (Egel, 1973; Egel and Egel-Mitani, 1974). The four haploid products of meiosis develop into ascospores. *S. pombe* is highly proficient for meiotic recombination. There are ∿45 crossovers per meiosis (Munz et al., 1989) distributed over only three chromosomes (Kohli et al., 1977). This results in an exceptionally high number of events per bivalent in comparison with other eukaryotes (King and Mortimer, 1990). Recently, many mutants specifically affecting meiotic recombination in *S. pombe* have been isolated (Ponticelli and Smith, 1989;

1. *Abbreviations used in this paper*: DAPI, 4′,6-diamidino-2-phenylindole; SC, synaptonemal complex; SPB, spindle pole body.

DeVeaux et al., 1992). Mutants with strongly reduced meiotic recombination show the low spore viabilities (~10%) that are expected for random segregation of the homologous chromosomes (Ponticelli and Smith, 1989). Thus, as in other eukaryotes (Baker et al., 1976), exchange events are probably necessary for proper chromosome segregation during meiosis I. In general, crossovers (and their cytological counterparts, the chiasmata) are not distributed randomly along and between the meiotic bivalents, an observation known as crossover interference (e.g., Jones, 1987; Carpenter, 1988). Interestingly, there is no crossover interference in *S. pombe* (Snow, 1979; P. Munz, manuscript submitted for publication). In *S. pombe* even the smallest chromosome (III) has on average eleven crossovers per bivalent in meiosis. Thus, even with random distribution of the exchange events, the probability that chromosome III remains without a crossover is extremely low.

Another peculiarity of fission yeast meiosis is the apparent lack of SCs (Olson et al., 1978; Hirata and Tanaka, 1982). Long filaments have been observed in sectioned meiotic nuclei, but little is known about their nature or function. In general, fission yeast meiosis, especially chromosomal structure and function, has hardly been characterized cytologically (Robinow and Hyams, 1989). It has been proposed that the SC is responsible for crossover interference (Egel, 1978; Egel-Mitani et al., 1982; King and Mortimer, 1990). This might explain why *S. pombe* shows no crossover interference. Similarly, *Aspergillus nidulans* also seems to lack SCs as well as crossover interference (Strickland, 1958; Käfer, 1977; Egel-Mitani et al., 1982). *A. nidulans* also shows exceptionally high frequencies of exchanges for all its eight chromosomes (Clutterbuck, 1992).

Probably much can be learned from *S. pombe* and *A. nidulans*. Structures like the observed linear elements might be derived from SC components and possibly have important functions for meiotic chromosome organization. They may help to define the functions of the SC and its components. For this reason, we have initiated an extensive analysis of *S. pombe* meiotic nuclei. Recently a method for spreading whole nuclei of budding yeast has been developed (Dresser and Giroux, 1988; Loidl et al., 1991), and we have now adapted this technique to fission yeast. The linear elements are clearly displayed in spread nuclei, and their morphology and time of appearance strongly suggest that they correspond to the axial cores of other eukaryotes. Tripartite SCs were not detected. A quantitative analysis of the elements in haploid, diploid, and tetraploid strains further suggests that the elements are connected to chromatin. From their high number it can be concluded that they are not formed continuously along the entire length of the chromosomes. Time course experiments revealed different prophase stages defined by length and arrangement of the elements. Nuclear morphology was analyzed in parallel by DNA staining and by serial thin sectioning. Time course experiments were also performed with strains blocked after S-phase due to the *mei4-B2* mutation (Bresch et al., 1968; Egel and Egel-Mitani, 1974). They accumulate at a late prophase stage. Recently, the *mei4* gene has been cloned and its gene product seems to bind DNA and is possibly a transcription factor (C. Shimoda and M. Yamamoto, personal communication). Sectioned nuclei revealed a constant configuration of the SPB (spindle pole body), the nucleolus, and the prospective cluster of centromeres nearby. Together with other data, this leads us to propose a mechanism that provides for a rapid initiation of chromosome pairing at the centromeres. Possible functions of the linear elements during meiosis are discussed and put in relation to the other experimental observations. Spreading allows the analysis of large numbers of nuclei by light and electron microscopy and is easily combined with genetic, molecular, and cytological approaches. It has been demonstrated in *Saccharomyces cerevisiae* that combined approaches are fruitful for unravelling the relationships between chromosome pairing, meiotic recombination, SC formation, and chromosome segregation (e.g., Giroux et al., 1989; Roeder, 1990; Loidl, 1991; Kleckner et al., 1991). A similar analysis of meiosis in fission yeast may contribute to the definition of the structural components and functions that are absolutely required for recombination and chromosome segregation, and give further insight into the complex events of meiotic prophase I.

Materials and Methods

Strains, Media, and Sporulation Conditions

The genotypes of the strains used in this study are listed in Table I. The diploid strains JB8 and JB9 were constructed as described by Gutz et al. (1974). These strains are prototrophic due to the interallelic complementing markers *ade6-M216* and *ade6-149* (Gutz, 1963). The haploid strain SP827 contains a *mat1* duplication with one stable *mat1-M* cassette as well as an inverted cassette that can switch between M and P information (A. Klar, personal communication). Cells which express M and P information simultaneously undergo meiosis in sporulation media. Cells which express only M information behave like h⁻ cells in crosses; this property was exploited to construct JB10. The tetraploid strain JB11 was constructed from two haploid strains with genotypes h⁻ *ade6-149 mei4-B2* and h⁺ *ade6-M216 mei4-B2*. In a first step, those strains were screened for colonies that had diploidized spontaneously and were homozygous for all three genetic markers. In a second step tetraploid cells were obtained from the two diploid strains in the same way as we obtained the strains JB8 and JB9, that is by mating the diploid strains and transferring the resulting zygotes to selective growth medium where only tetraploid cells with the interallelic complementing *ade6* alleles can grow. JB11 is not a stable strain and has to be constructed and checked for cell size immediately before each experiment.

Standard genetic methods and media were as described by Gutz et al. (1974). To obtain meiotic cultures, single colonies were grown in yeast extract medium (supplemented with 6.7 g/liter Difco nitrogen base for tetraploids) to stationary phase. The cells were then diluted 1:100 in the synthetic minimal medium PM (*S. pombe* minimal; Beach et al., 1985) and grown at 30°C with shaking to a titer of 1×10^7 cells/ml. The cultures were screened for efficient sporulation and cell morphology in parallel. The selected culture was harvested by centrifugation, washed once in PM-N (PM without NH₄Cl; Watanabe et al., 1988), and resuspended in the same volume of PM-N. Sporulation was performed under vigorous shaking (200 rpm) at 30°C. The same sporulation protocol was used for the homothallic haploid strains (968 and mei4) with a few alterations. The cells were grown in PM to a titer of 2×10^7 cells/ml, harvested by centrifugation, and diluted to 5×10^6 cells/ml in PM-N without washing. Under these conditions the first zygotes appeared after 5 h in PM-N.

Time Course Experiments

The cells were prepared for time course experiments as described in the sporulation protocol above. A 200-ml PM culture was partitioned into a 25-ml PM-N culture (in a 125 ml flask) and a 175-ml PM-N culture (in a 1 liter flask). The 25-ml culture was used to measure replication by 6-³H-uracil labeling of DNA as described by Szankasi and Smith (1992). In control cultures with 0.2 M hydroxyurea in the medium, no DNA replication was detected. The 175-ml culture was used to analyze the other meiotic events. Commitment to meiosis was measured by plating appropriate dilutions of cells at hourly intervals onto yeast extract plates. On this medium diploid cells grow as white colonies due to interallelic complementation of

Table I. List of Strains

Strain	Genotype	Source
968	h^{90} (homothallic wild-type)	U. Leupold‡
mei4	h^{90} mei4-B2	U. Leupold‡
JB8	h^+/h^- ade6-M216/ade6-149	This study
JB9	h^+/h^- ade6-M216/ade6-149 mei4-B2/mei4-B2	This study
SP827	mat1-M smt-O::mat1 ade6-M210	A. Klar*
JB10	mat1-M smt-O::mat1 mei4-B2	This study
JB11	$h^+/h^+/h^-/h^-$ ade6-M216/ade6-M216/ade6-149/ade6-149 mei4-B2/mei4-B2/mei4-B2/mei4-B2	This study

* NCI-Frederick Cancer Research and Development Center, Laboratory of Eukaryotic Gene Expression, Frederick, MD.
‡ Institute of General Microbiology, University of Bern, Bern, Switzerland.

ade6-M216 and ade6-149 whereas haploid adenine auxotrophic cells, containing only one of the two ade6 mutations, will yield pink colonies. Thus, the fraction of pink colonies reflects the percentage of cells having been committed to meiosis at the time of plating. To spread the nuclei, aliquots of cells were harvested 20 min before each time point to take into account that progress of meiosis might continue during digestion of the cell wall. Mature spores can not be spread. Their percentage was determined by phase contrast microscopy at each timepoint and taken into account for the statistical evaluation of the nuclei examined in the EM. For staining of the cells with DAPI (4',6-diamidino-2-phenylindole, DNA staining agent) 1 ml of cell culture was centrifuged briefly, fixed with an equal volume of ice-cold 70% ethanol and stored overnight at 4°C. 100 μl of fixed cells were then added to 1 ml of ice-cold PBS, centrifuged, and resuspended in a solution of DAPI (200 ng/ml).

Whole Mount Spreading of Meiotic Nuclei

For the digestion of the cell wall 10 ml of a meiotic culture were harvested by centrifugation and resuspended in 2 ml of 0.65 M KCl containing 10 mM DTT, 50 μg/ml Zymolyase 100 T (ICN Biomedicals, Inc., Costa Mesa, CA) and 5 mg/ml Novozym 234 (Novo Nordisk Biolabs, Denmark). After 30–45 min at 30°C and gentle shaking, digestion of the cell wall was almost complete (more than 90% protoplasts). The longer the cells remain in meiotic medium the more resistant they become to cell wall digestion. The protoplasts were harvested by gentle centrifugation, washed once with ice-cold 0.1 M MES (2-[N-morpholino] ethanesulphonic acid) pH 6.4/1 M sorbitol/1 mM EDTA/0.5 mM MgCl$_2$ and resuspended in the same solution to an appropriate density for spreading ($\sim$500 μl). In this solution the protoplasts can be kept on ice for several hours before spreading. Immediately before spreading, 1 μl of a 1 M PMSF (phenylmethylsulfonyl fluoride) solution in dimethyl sulfoxide was added to the protoplasts.

Spread nuclei were prepared and stained as described by Loidl et al. (1991) with some alterations. Briefly, 20 μl of protoplast suspension were put on a cleaned slide, 40 μl fixative (4% wt/vol paraformaldehyde unbuffered, 3.4% sucrose) and 80 μl Lipsol (L. I. P. Ltd., Shipley West Yorkshire, England) were added and immediately mixed. A second addition of 80 μl fixative followed after about 30 s and the suspension was evenly distributed on the slide with a glass rod. The protoplast suspension, the fixative, and the Lipsol were all kept on ice for spreading. The interval before the second addition of fixative was shortened or extended to get weaker or stronger spreading conditions, respectively. After drying overnight, the slides were put in 0.2% vol/vol Photo-Flo (Eastman Kodak Co., Rochester, NY) with gentle shaking for $\sim$20 s to remove the sticky sucrose layer. The slides were covered again with fixative for 10 min, rinsed with 0.2% Photo-Flo, and air dried for at least 3 h.

For silver staining, a few drops of an aqueous 50% silver nitrate solution were pipetted on the slides, covered with a piece of nylon tissue, and incubated at 60°C for 1 h in a moisture box. The stained slides were rinsed with water, shortly dipped in 0.2% Photo-Flo, and air dried. The slides were covered with a thin plastic film (0.75% wt/vol polystyrol in chloroform) and prescreened by light microscope (magnification of 100) for suitable areas which were marked with a pen. The film with the spread nuclei was detached from the slide by adding some drops of 1% hydrofluoric acid (caution, as hydrofluoric acid is very corrosive). The promising areas were transferred to 50 mesh copper grids. The nuclei were examined with a Philips EM300 at 60 kV (Philips Eindhoven, The Netherlands).

Serial Sections

Samples were fixed in 3% glutaraldehyde, treated with Zymolyase, postfixed in 2% OsO$_4$, stained in uranyl acetate, and processed as described by Hirata and Tanaka (1982). Serial sections were picked up with unfilmed single slot grids, stained with lead citrate (Reynolds, 1963), and mounted on Formvar films as described by Rowley and Moran (1975). During sectioning, the cohesion of the ribbons was achieved by coating of the block with contact cement (Fahrenbach, 1984).

Results

Spread Meiotic Nuclei of S. pombe Reveal Structures Resembling Axial Cores of Other Eukaryotes

Diploid cells of the strain JB8 were sporulated and nuclei were spread at times when most of them were expected to be in meiotic prophase I (5–7 h after meiotic induction). To spread S. pombe nuclei, we adapted a spreading technique worked out for S. cerevisiae, followed by silver staining and analysis with the electron microscope (see Materials and Methods). In these preparations the nucleolus and the SPB are densely stained by silver nitrate, whereas the chromatin appears as a fuzzy mass of medium electron density. Nuclei spread during meiotic prophase often contain densely staining "linear elements" embedded in the chromatin mass (Fig. 1, b–h) which were absent in nuclei of other stages (Fig. 1, a and i). The thickness, staining behavior, and general morphology of these elements is strongly reminiscent of the axial elements in other organisms. With regard to the linear elements we could distinguish several classes of spread nuclei. Some nuclei showed few and very short elements (class I, Fig. 1, b and h). In another class of nuclei, the elements seemed to contact each other or to be entangled with each other so that extensive networks of elements were formed (class IIa, Fig. 1, c and d). Some nuclei even contained bundles with several elements closely aligned (class IIb, Fig. 1, e and f). In yet other nuclei, we observed many dispersed long elements, showing hardly any contact to each other (class III, Fig. 1 g). In some preparations the chromatin was less evenly spread out and seemed to be anchored on both sides to the linear elements, resembling the chromatin loops of axial elements and SCs (Fig. 2 a; Rattner et al., 1980, 1981; Weith, 1985). However, we never discovered any regular tripartite structures which are typical for the SC found in most eukaryotes. When we applied the same spreading technique to S. cerevisiae tripartite SCs could easily be detected (Fig. 2 b).
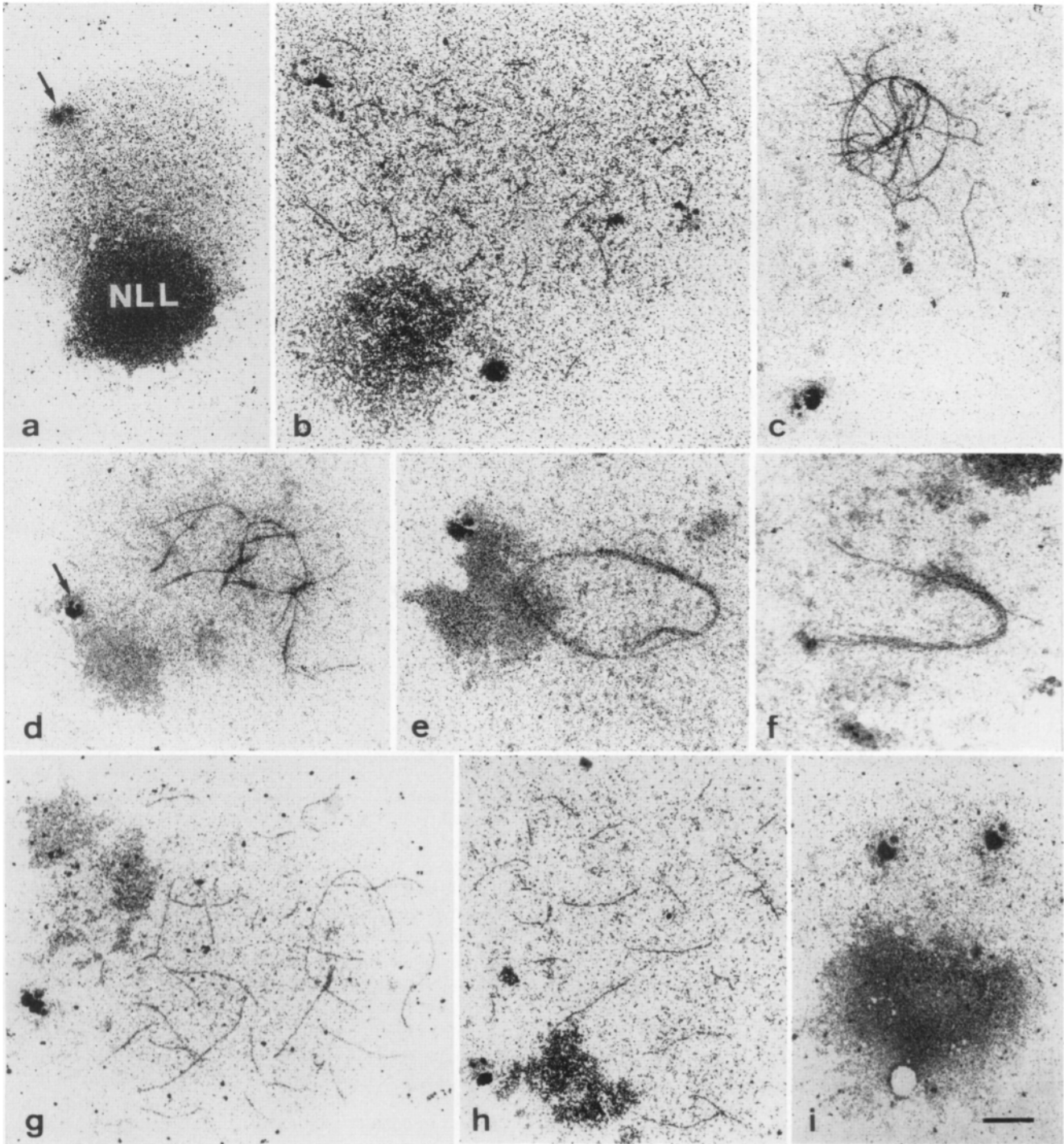
Figure 1. Electron micrographs of spread and silver-stained nuclei of the diploid standard strain JB8 showing the changes in nuclear morphology during meiosis. (*a*) Vegetative cell before induction of meiosis. The nucleolus (*NLL*) and a duplicated SPB (*arrow*) are clearly visible. The nucleolus is more compact than in meiotic cells. (*b*) Early prophase nucleus of class I (stage 1) revealing several short segments of linear elements. (*c*) Nucleus of class IIa with elements entangled to a network. The nucleolus is sometimes absent during this stage. (*d*) Another example of a class IIa nucleus. Elements contact each other at some regions. The SPB (*arrow*) is close to the nucleolus and consists of one big and two small bodies (see also *e*, *g*, and *h*). (*e*) Nucleus of class IIb with elements closely aligned. (*f*) Bundle of several elements in a class IIb nucleus. (*g*) Nucleus of class III with several long and single linear elements. (*h*) Late prophase nucleus of class I (stage 4). The elements become shorter again before they completely vanish. (*i*) Post-prophase nucleus showing a separated SPB. The two daughter SPBs are duplicating again in preparation for the second meiotic division (small adjacent bodies). Bar, 1 μm.
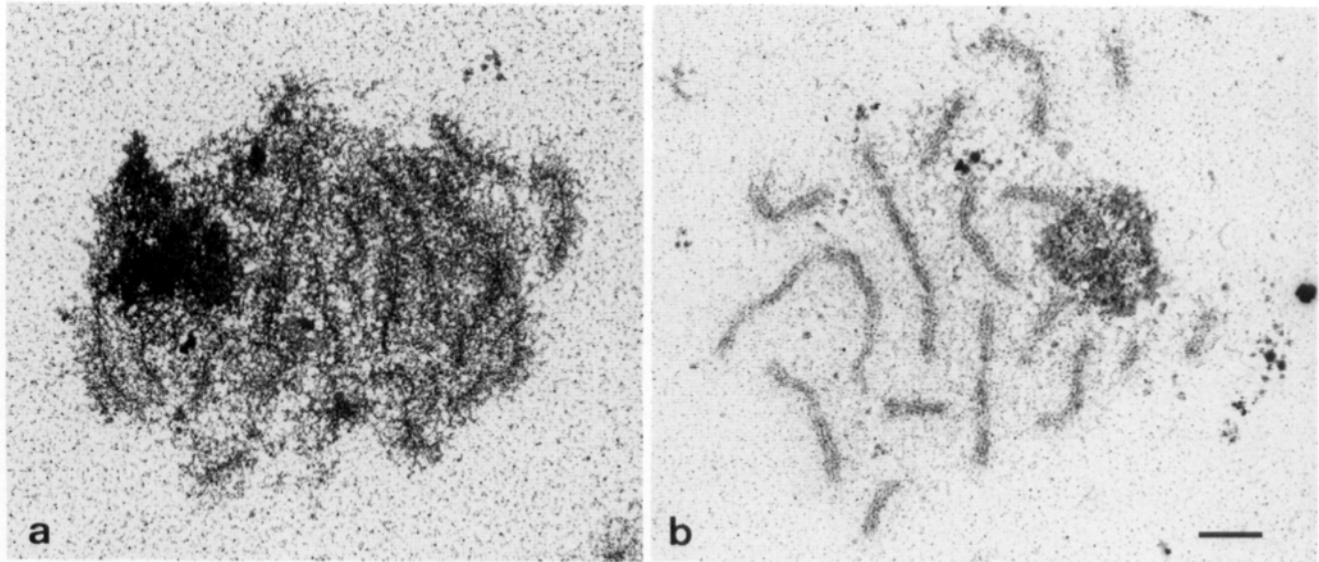
Figure 2. (*a*) Spread and silver-stained nucleus of *S. pombe* with chromatin loops apparently attached to the linear elements. (*b*) Spread and silver-stained nucleus of an SK-1 strain of *S. cerevisiae*. Pachytene stage revealing the tripartite structure of the SCs. The same spreading method was used as for *S. pombe* nuclei. Bar, 1 μm.

Timing of Cytological Events of Meiosis

To investigate whether the different classes of spread nuclei show a defined sequence, that is whether they represent different meiotic stages, we performed time course experiments. For comparison with other meiotic events, we determined DNA synthesis, commitment to meiosis, and the meiotic divisions in the same experiments. We also analyzed changes in the shape of meiotic prophase nuclei by DAPI staining. Such time course experiments were repeated four times totally, yielding qualitatively identical results. When cells were shifted with a lower titer than 10^7 per ml, all meiotic events were significantly delayed.

The diploid standard stain JB8 was induced to undergo meiosis and nuclei (taken at hourly intervals) were spread, silver stained and classified in the electron microscope (see Materials and Methods, Fig. 3 *a*). The following temporal order of four prophase stages was deduced: at first short elements appear (class I nuclei) being defined as stage 1. Subsequently, the elements grow and form the networks and bundles typical for nuclei of classes IIa and IIb, respectively (stage 2). Later, the nets and bundles seem to dissociate to single and long elements (stage 3). These elements then seem to disintegrate again (stage 4), as judged by the renewed increase of class I nuclei with coincident decrease of class III nuclei after 7 h (Fig. 3 *a*). It is possible to estimate the duration of each stage by determination of the area under the corresponding curve which is then divided by the total percentage of cells undergoing meiosis (Padmore et al., 1991). This percentage of active cells was evaluated from the percentages of cells being committed to meiosis and having completed the first meiotic division 12 h after induction of meiosis (85%). 20 h after induction, 90% of the cells had completed sporulation. It has to be borne in mind that nuclei of class I do not represent a homogeneous stage but represent two stages (stages 1 and 4), as concluded from the biphasic curve for class I nuclei (Fig. 3 *a*). When the class I curve was resolved into two curves, durations of ∿0.75 and 0.5 h

were estimated for stages 1 and 4, respectively. The stages 2 and 3 last about 1 and 1.25 h, respectively.

Fig. 3, *b* and *c*, show the relations between premeiotic DNA synthesis, commitment to meiosis, first meiotic division, and the classes of nuclei observed by light and electron microscopy. The timing of commitment to meiosis (the developmental point where cells have irreversibly entered meiosis, see Materials and Methods), and the timing of the completed first meiotic division (determined by the percentage of cells containing at least two DAPI stainable bodies) is shown in Fig. 3 *b*. In addition the DAPI-stained nuclei are classified according to their shape which shows distinct changes during meiotic prophase (Fig. 4). The following types of prophase nuclei can be distinguished. Some nuclei are hook or pear shaped and were designated as deformed nuclei (Fig. 4, *c* and *e*). Other nuclei show a very prominent elongation, a stage similar to the one described by Robinow (1977) as "horse tail" nuclei (Fig. 4 *d*). Sometimes it is possible to detect longitudinal filamentous structures in these nuclei probably corresponding to chromatin fibers. Under the assumption that the deformed and horse tail nuclei are true prophase stages, we obtained stage durations of ∿0.3 and 0.5 h, respectively. For a better temporal comparison the noncumulative curves of the deformed and horse tail nuclei were integrated to cumulative curves with the use of the estimated stage durations (as described by Padmore et al., 1991). The cumulative curves show the proportion of cells having entered the stage of interest. They parallel nicely the curves of commitment and first meiotic division and reveal that the deformed nuclei appear ∿1 h before the horse tail nuclei. The most abundant class of meiotic prophase nuclei are those designated as elongated nuclei (Fig. 4, *b* and *e*). They show an elongation which clearly distinguishes them from vegetative nuclei, but it is less prominent than in the horse tail nuclei. Besides that, elongated nuclei stain more intensely with DAPI than horse tail nuclei. The elongated nuclei are also detected in mitotic prophase (possibly corre-
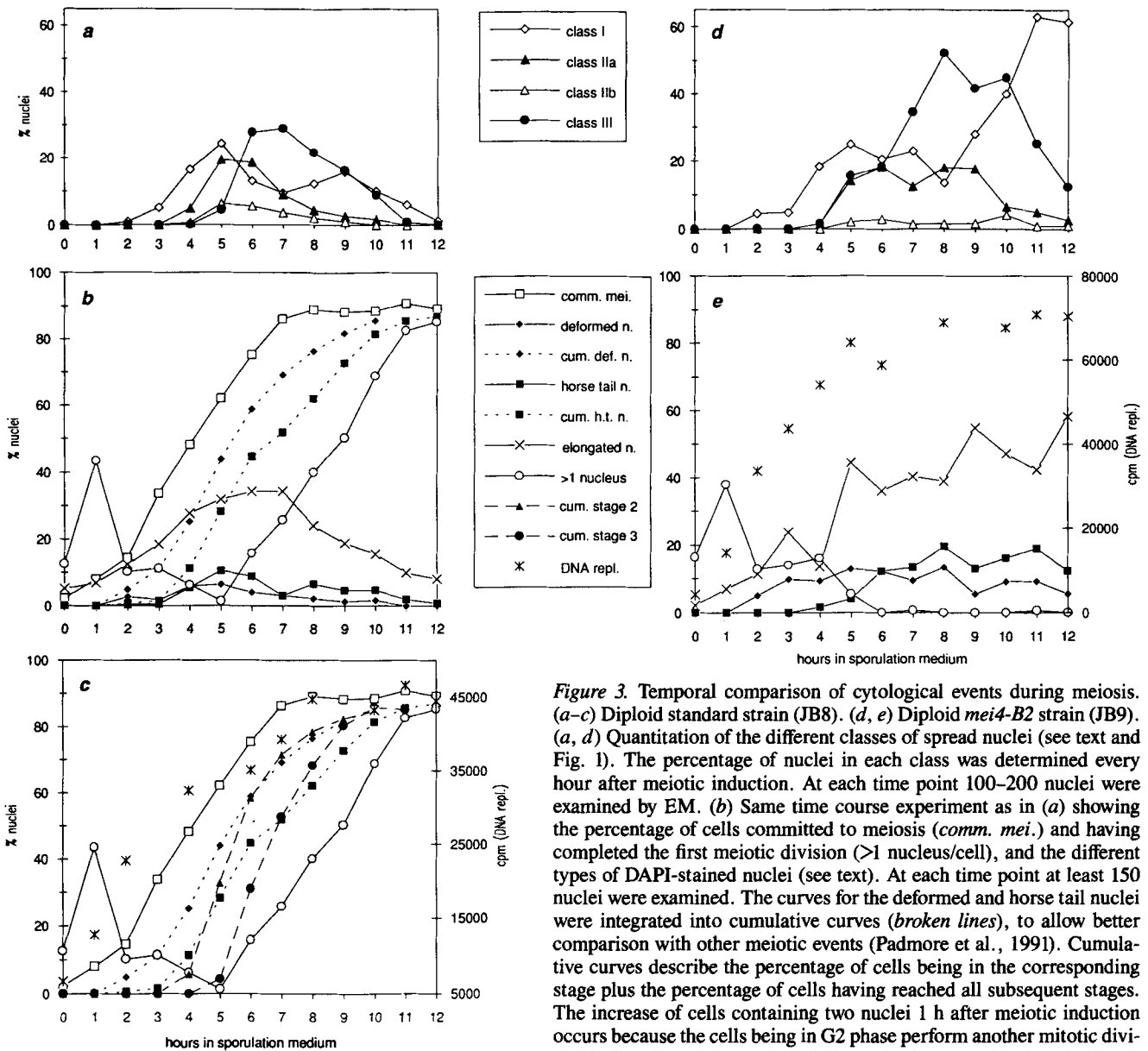
Figure 3. Temporal comparison of cytological events during meiosis. (*a–c*) Diploid standard strain (JB8). (*d, e*) Diploid *mei4-B2* strain (JB9). (*a, d*) Quantitation of the different classes of spread nuclei (see text and Fig. 1). The percentage of nuclei in each class was determined every hour after meiotic induction. At each time point 100–200 nuclei were examined by EM. (*b*) Same time course experiment as in (*a*) showing the percentage of cells committed to meiosis (*comm. mei.*) and having completed the first meiotic division (>1 nucleus/cell), and the different types of DAPI-stained nuclei (see text). At each time point at least 150 nuclei were examined. The curves for the deformed and horse tail nuclei were integrated into cumulative curves (*broken lines*), to allow better comparison with other meiotic events (Padmore et al., 1991). Cumulative curves describe the percentage of cells being in the corresponding stage plus the percentage of cells having reached all subsequent stages. The increase of cells containing two nuclei 1 h after meiotic induction occurs because the cells being in G2 phase perform another mitotic division before they can enter meiosis from G1 phase (Egel and Egel-Mitani,

1974). (*c*) Direct temporal comparison of DNA replication, commitment to meiosis, and first meiotic division with the cumulative (*cum.*) curves which were integrated from the corresponding noncumulative curves of the different types of nuclei detected by EM analysis and fluorescence microscopy (*a* and *b*). Subclasses IIa and b were pooled for the cumulative curve (stage 2). The curve of class I nuclei was not integrated because it represents two different stages (see text). DNA replication was measured by ³H labeling and is indicated in cpm/2 ml sample. (*e*) Same time course experiment as in (*d*) showing DNA replication, the percentage of cells with 2 nuclei, as well as the timing of the different types of DAPI-stained nuclei (see text and *b*). At least 100 nuclei were examined from each time point.

sponding to the compact form described by Toda et al., 1981) which explains that there are some elongated nuclei at the time of meiosis induction (0 h). All types of prophase nuclei can be clearly distinguished from vegetative interphase nuclei (Fig. 4 *a*).

Fig. 3 *c* compares DNA replication (see Materials and Methods), commitment to meiosis, and first meiotic division with the cumulative curves of nuclear classes observed in the fluorescence and electron microscope. The cumulative curves are derived from the curves of element classes II and III observed in spread nuclei and from the deformed and horse tail types of nuclei found by DAPI staining. Premeiotic DNA

replication and commitment to meiosis closely coincide (as described earlier by Beach et al., 1985). The different stages of meiotic nuclei revealed by electron and fluorescence microscopy all appear at times expected for prophase I nuclei, that is after S-phase and before the first meiotic division. Nuclei of classes IIa and b (stage 2) were pooled to generate the cumulative curve. When they are integrated separately, class IIa nuclei appear shortly before IIb nuclei (data not shown). Stage 3 starts ∼1 h after stage 2. The cumulative curves from the EM analysis show a faster increase than the other cumulative curves, particularly in their lower part. This derives from the asymmetry of the noncumulative curves

246

being steeper at their left half (Fig. 3 *a*). We do not know the reason for this bias, but it probably reflects technical differences in the evaluation of data from the electron microscope and the other experiments. Therefore, the times where 50% of the active cells have entered the corresponding stages should be the most reliable points for comparison. It seems that the nuclei are deformed during stage 2 and that the horse tail nuclei are temporally correlated to stage 3 (see also Discussion).

We also observed the behavior of the SPB during meiotic development (spread nuclei). At the time of meiotic induction (0 h), ~60% of the nuclei contained duplicated but unseparated SPBs (Fig. 1 *a*), whereas 33 and 7% of the nuclei showed single or separated SPBs, respectively. The number of cells containing a single SPB increased significantly before the first elements appeared. Nuclei showing elements revealed a silver-staining body with two adjacent smaller bodies near the nucleolus (Fig. 1, *d, e, g, h*). The diameter of the big body was ~300 nm which corresponds to the diameter of the SPB determined in sections of nuclei containing elements (see below). After disappearance of the elements, the SPB first appeared duplicated but unseparated and was no longer connected with the nucleolus. A separated SPB is shown in Fig. 1 *i*. These meiotic SPBs are bigger than the mitotic SPBs (compare Fig. 1, *a* with *i*). At later stages we often found three or four very prominent bodies tied together (not shown) which probably represent the multi-layered differentiated SPB organizing the forespore membrane (Tanaka and Hirata, 1982). The changes in nucleolar structure during meiotic development are described in the legend to Fig. 1.

Timing of Cytological Events in a mei4-B2 Mutant Strain

Strains containing the *mei4-B2* mutation are blocked after

S-phase but before the first meiotic division (Egel and Egel-Mitani, 1974; Olson et al., 1978; Shimoda et al., 1985). For a comparison, we performed time course experiments with the diploid strain JB9 (homozygous for *mei4-B2*) in the same way as described for the standard diploid strain JB8 (see above). The timing of the different classes of spread meiotic nuclei is indicated in Fig. 3 *d*. Again, nuclei of class I precede the other stages. In this experiment nuclei of classes II and III appear at about the same time, but class III nuclei peak 2 h later at almost twice the level as compared to the standard strain. After 8–10 h in sporulation medium, the single elements become shorter corresponding again to class I nuclei. 30 h after induction of meiosis only very few short elements remained in the nuclei (data not shown). Thus, *mei4-B2* cells accumulate predominantly in late prophase stages that contain single linear elements. The time course of the *mei4-B2* meiosis was studied in four independent experiments yielding qualitatively identical results.

Fig. 3 *e* shows the timing of the different types of nuclei obtained by DAPI staining in the same time course experiment and in the same way as described for the standard strain. DNA replication and cells containing two nuclei are also indicated. No cells with two or more nuclei were detected in late stages. As in wild-type meiosis, the deformed nuclei seem to appear slightly earlier than the horse tail nuclei and cells become predominantly (but not exclusively) enriched with horse tail and elongated nuclei. The number of elongated nuclei increases before the appearance of short elements, immediately after induction of meiosis (as in wild-type meiosis, Fig. 3 *b*). The enrichment for prophase nuclei is transient, because 30 h after induction of meiosis the nuclei are roundish or only slightly elongated (not shown, see also Olson et al., 1978). Under meiotic conditions, *mei4-B2* strains show all the types of nuclear shapes and spreading classes that are detected in standard cells (Fig. 5). Furthermore, the sequence of the stages deduced from wild-type
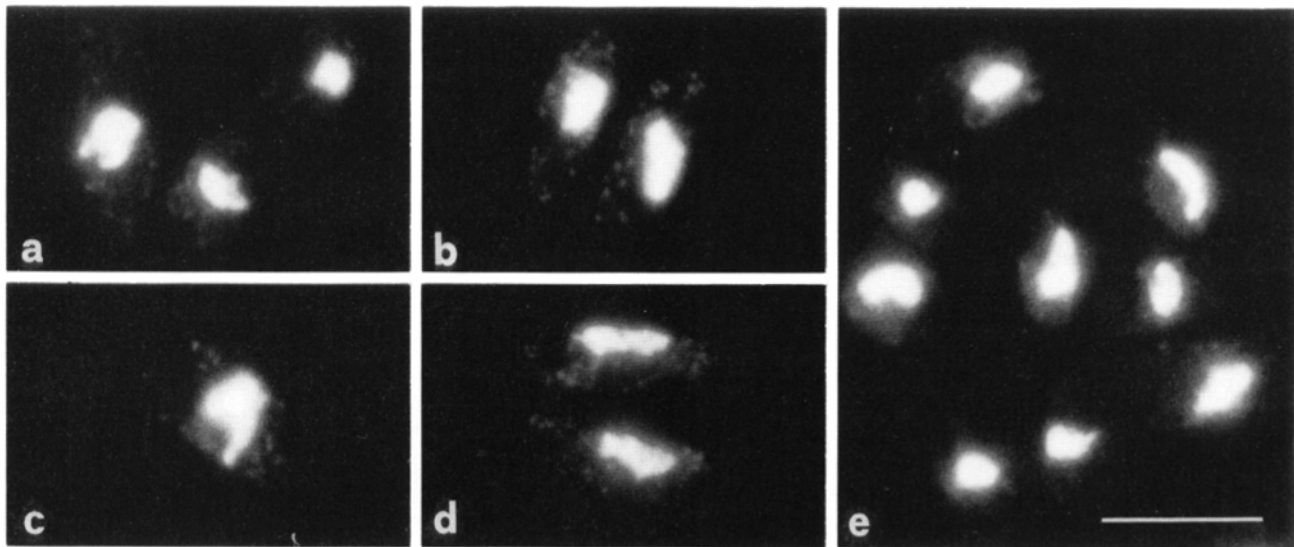

Figure 4. DAPI staining of meiotic diploid cells. (*a*) Vegetative cells at the time of meiotic induction. The left nucleus shows the typical appearance of interphase chromatin, with a hemispherical region and two small protrusions (nucleolar organizer region, Toda et al., 1981). The cell on the right contains a mitotically divided nucleus. (*b*) Elongated nuclei. (*c*) Deformed nucleus. (*d*) Horse tail nuclei, filamentous appearance of the chromatin is apparent when directly observed by microscope (see also Robinow, 1977). (*e*) Deformed (hook- and pear-shaped) nuclei and elongated nuclei. Bar, 10 μm.
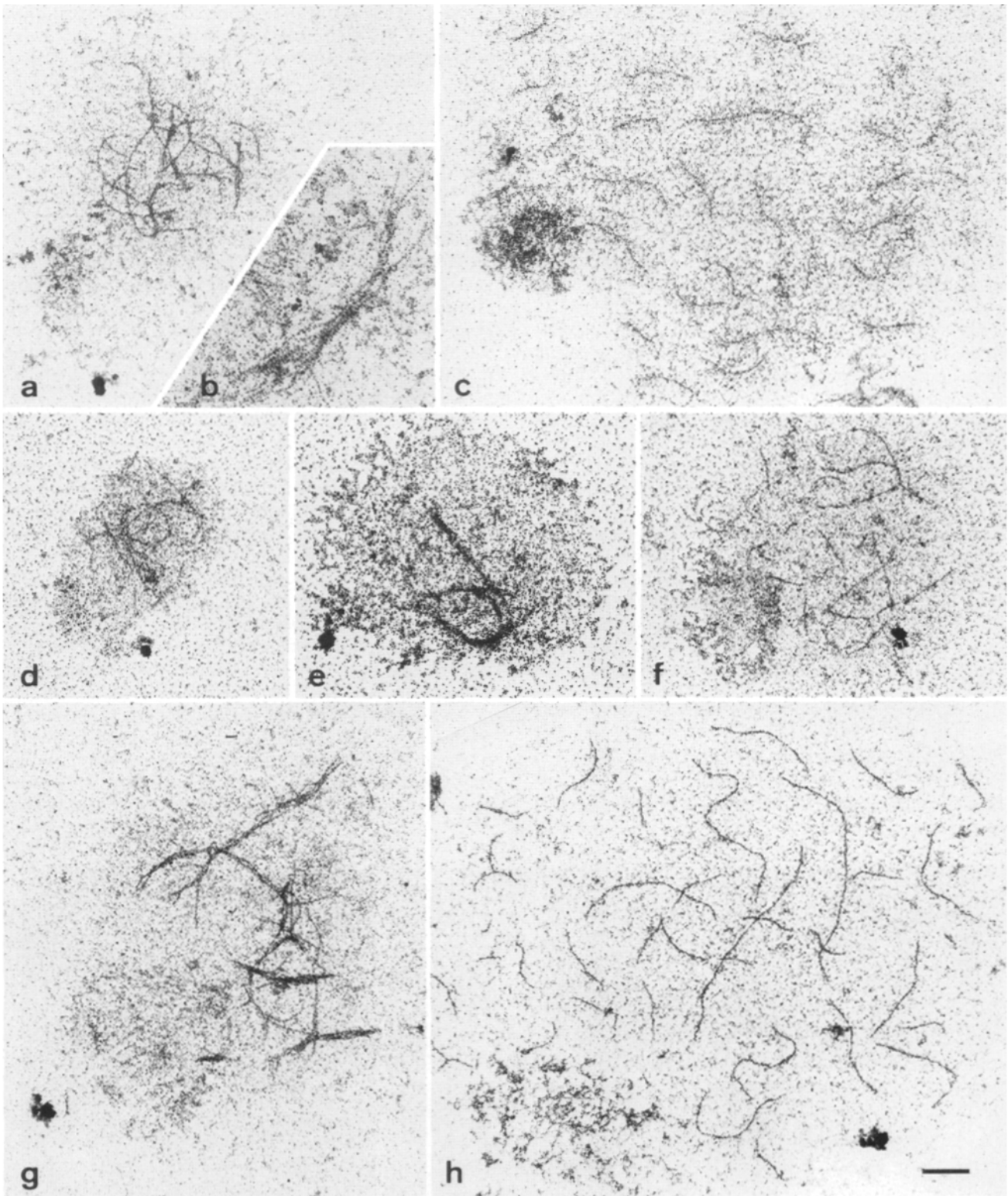
Figure 5. Electron micrographs of spread and silver-stained nuclei of diploid, haploid, and tetraploid *mei4-B2* strains. (*a–c*) Diploid strain (JB9). (*a*) Nucleus of class IIa. (*b*) Bundle of several elements in a class IIb nucleus. (*c*) Nucleus of class III. (*d–f*) Haploid strain (JB10). (*d*) Nucleus of class IIa. (*e*) Nucleus of class IIb. (*f*) Nucleus of class III. (*g* and *h*) Tetraploid strain (JB11). (*g*) Nucleus of class IIa. (*h*) Nucleus of class III. Bar, 1 μm (*a*, *c–h*), 1.7 μm (*b*).

meiosis is also observed in the *mei4-B2* cells up to the strong delay in stage III.

Sporulation and Spreading of Homothallic and Heterothallic Strains

As a haplontic organism, *S. pombe* normally enters meiosis directly after fusion of two cells with different mating-types. Therefore, we also examined spread nuclei from such a zygotic meiosis. We sporulated the haploid homothallic strains 968 (wild-type) and mei4 (*mei4-B2*) as described in Materials and Methods. These strains reveal the same classes of spread and silver-stained nuclei as those described from the azygotic meiosis of diploid strains. In the strain mei4 we also classified 120 nuclei at 8, 10, and 12 h in sporulation medium. Of the nuclei containing elements, 66% were of class II at 8 h. The remaining 34% of nuclei contained single elements (class I and III). These percentages gradually changed to 32% of class II nuclei and 68% of class I and III nuclei at 12 h. Thus, the behavior of the linear elements and their temporal sequence (associated elements before single elements) do not seem to be a peculiarity of an azygotic meiosis in diploid strains.

As a further control, we shifted the haploid heterothallic strains 972 (h^-) and 975 (h^+) separately to meiotic conditions and examined spread nuclei at different time points. Due to the lack of a mating partner these strains are not able to sporulate. We could not detect any elements in these strains, at time points when strain 968 contains an abundance.

Quantitation of the Linear Elements in Strains with Different Ploidy

To further investigate a possible correlation of the linear elements with chromosomes, we determined the number and length of the elements in haploid, diploid, and tetraploid strains. We chose *mei4-B2* strains for this investigation because they become highly enriched for class III nuclei with single long elements (Fig. 3 *d*). The haploid strain JB10 is a derivative of SP827 which is able to sporulate in the haploid state due to a duplication of mating-type information (see Materials and Methods). The diploid strain JB9 was the one used for the time course experiments. The tetraploid strain JB11 formally contains twice the information of JB9 (for construction see Materials and Methods). These three

strains were induced to enter meiosis and nuclei were spread and silver-stained 5 and 9 h later. It is important to note that all the classes of spread nuclei observed in diploid strains (Fig. 1) could also be detected in the haploid and the tetraploid strain (Fig. 5). From all strains, at least 40 pictures were taken of nuclei showing strikingly many and/or long single elements. The pictures were visually preselected for abundant elements and the length of the elements was determined with a digitizer in 20 pictures of each strain. This selection guarantees that mainly those nuclei were taken into account that had maximally developed elements and thus, were at comparable stages. The results are given in Table II. The mean total length of the elements per nucleus correlates well with the ploidy of the strains, differing approximately by a factor of two. However, the mean numbers of elements per nuclei differ by less than a factor of two and there is an overlap of the extreme values. Thus, the mean length of the elements is slightly shorter in haploids and larger in tetraploids. Nevertheless, there is a significant rise in the element number with increasing ploidy. In all strains the number of elements shows no direct correlation to the number of chromosomes in fission yeast ($n = 3$).

From 80 nuclei measured by digitizing, 46 (57.5%) showed an even number of elements, which is not significantly different from 50%. There was no correlation between the number of elements per nucleus and the total element length per nucleus. However, there was a clear negative correlation between the number of elements per nucleus and the mean length of elements in the same nucleus, which means that nuclei with many elements tend to have shorter elements than nuclei with less elements (data not shown). We do not think that this is an indication of fragmentation of the elements during the spreading process (see Discussion). There do not seem to exist discrete lengths of elements because we obtained a continuous range of values. The distributions of element lengths in the three strains are illustrated in Fig. 6. These distributions show a shift to longer elements with increasing ploidy. Most elements measure ∼1 μm, with only a few being much shorter. The same distribution of element length is observed within single nuclei; there are no pairs of elements with the same length.

We also measured spread meiotic nuclei of the standard diploid strain (JB8). In the nuclei with the highest amount of elements, the total element length per nucleus and the mean number of elements per nucleus reached comparable

Table II. Number and Length of the Linear Elements in Haploid, Diploid, and Tetraploid Strains

Strain (ploidy)	Mean sum of element length/nucleus	Factors	Mean number of elements/nucleus	Factors	Mean length of elements	Factors
	μm				*μm*	
JB10 (1n, *mei4-B2*)	18.7 ± 1.9 (16.2 to 22.3)	0.55	15.1 ± 2.3 (12 to 20)	0.62	1.24 ± 0.89 (0.18 to 5.58)	0.88
JB9 (2n, *mei4-B2*)	34.3 ± 2.5 (30.0 to 39.6)	1.00	24.4 ± 3.0 (18 to 30)	1.00	1.41 ± 0.88 (0.19 to 5.17)	1.00
JB11 (4n, *mei4-B2*)	66.9 ± 7.7 (54.6 to 83.0)	1.95	34.4 ± 6.2 (24 to 48)	1.41	1.95 ± 1.38 (0.24 to 7.87)	1.38
JB8 (2n, *mei4⁺*)	33.3 ± 4.9 (28.0 to 42.2)	0.97	21.8 ± 4.7 (19 to 23)	0.89	1.53 ± 1.07 (0.25 to 7.91)	1.09

The average values are indicated with the corresponding standard deviation. The extreme values are given in parentheses. The factors show the relative difference in the mean values with reference to the diploid strain JB9. 20 nuclei of the *mei4-B2* strains and six nuclei of the standard strain were considered. The total number of elements measured were 301, 488, 687, and 131 for JB10, JB9, JB11, and JB8, respectively.
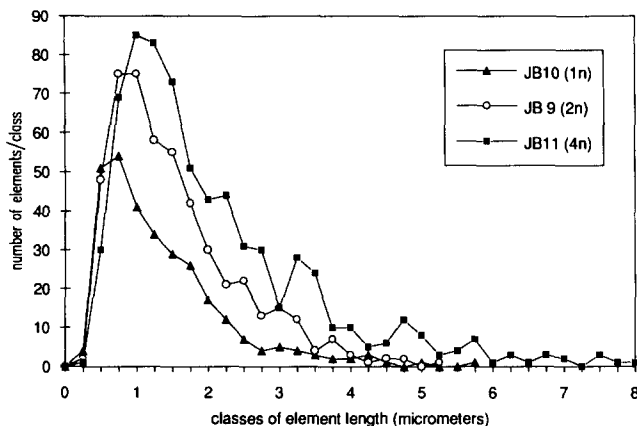
Figure 6. Distribution of element lengths in haploid, diploid, and tetraploid *mei4-B2* strains. The elements from all nuclei were grouped in classes of 0.25 μm (0–0.25, 0.25–0.5 . . . 7.75–8.0 μm). The number of elements counted in each class is compared in the strains with different ploidy.

values as in the diploid *mei4-B2* strain JB9 (Table II). Thus, in the arrested prophase nuclei of *mei4-B2* strains the elements do not seem to become additionally elongated in comparison with the standard strain.

Serial Thin Sectioning of Meiotic Nuclei

As a complementary approach we also prepared serial sections of meiotic nuclei of the diploid standard strain JB8 to gain further insight into the nature and three-dimensional arrangement of the linear elements. We could distinguish at least two types of nuclei with elements. Some nuclei were more or less elliptical or had strikingly deformed shapes. In these nuclei short segments of elements appeared, mostly without a defined direction or order (Fig. 7, *a* and *b*), but sometimes following the curvature of the nuclear membrane (Fig. 7, *c–g*). In these nuclei, parallel alignment of two elements over short stretches or indications of interconnections are often visible. The elements seem either to be short or extensively twisted. They were nearly impossible to follow in three-dimensional reconstructions. These nuclei probably correspond to stage 1 (short elements) and stage 2 (networks, bundles) of spread nuclei. According to their shape, they obviously correspond to elongated and deformed nuclei observed by DAPI staining.

The other type of nuclei observed in sectioned material were elongated with several single elements running in ordered arrays mainly parallel to the long axis of the nucleus (Fig. 7 *i*). These nuclei have been described previously (Olson et al., 1978) and it has been shown that a *mei4-B2* strain is blocked at this stage. Thus, these nuclei most probably correspond to stages 3 and 4 of spread nuclei (single long or short elements, respectively). The elements showed the greatest order in parallel arrays in those nuclei being most extensively stretched out (designated as horse tail nuclei). The stretched shape of these nuclei seems to be stabilized by a bundle of microtubules running longitudinally outside the nuclear membrane (Olson et al., 1978, and our observations). Three-dimensional reconstructions of such nuclei yielded ~20 linear elements with no indications of continuity between them. Although the elements were difficult

to observe in cross-sections, it was nevertheless possible to follow them over several sections in some of the series. We never observed elements being connected with the nuclear membrane.

In each serially sectioned nucleus we observed two or three "black bodies" that differed in size (Fig. 7, *b–d*, *l*). The diameter of the largest body was ~150 nm. In 10 out of 12 nuclei of which all sections were studied, the nucleolus, the SPB, and the black bodies showed a typical arrangement with the SPB adjacent to the nucleolus and the black bodies facing the SPB at some distance (Fig. 7 *h*). This configuration was observed in both types of sectioned nuclei described above. We suggest that the black bodies represent the centromere regions of the three chromosomes (see Discussion). Linear elements are not connected with the black bodies. Some nuclei contained a striking "round body" close to the nucleolus (Fig. 7 *k*). Such round bodies were also observed in spreads of late stages of meiosis (not shown). We assume that they represent some kind of nucleolar differentiation as also observed in other organisms (e.g., Dresser, 1987, and references cited therein).

Discussion

In this study we have analyzed meiotic prophase in fission yeast with different cytological approaches. We try to interpret the data on meiotic chromosome structure and behavior with respect to pairing and segregation of homologous chromosomes.

Characteristics of Meiotic Prophase in Fission Yeast

In spreads and serial sections of prophase I nuclei we have observed long filaments that were described before by Olson et al. (1978) as "linear elements". We propose that they correspond to the axial cores of other eukaryotes and connect two sister chromatids. This conclusion is suggested both by their morphology (Figs. 1, 2, and 7) and by their time of occurrence (Fig. 3). We consider it unlikely that the linear elements are formed separately along each single chromatid or that they reflect synapsed chromosomes and correspond to central elements. By shifting a diploid strain from growth medium to sporulation medium (see Materials and Methods), it is possible to obtain quite synchronous meiotic cells. To time the appearance of the linear elements relative to other meiotic events, we also followed premeiotic DNA replication, commitment to meiosis, and the meiotic divisions in time course experiments (Fig. 3, *a–c*). The elements appear at the time expected for meiotic prophase. All stages showing elements last together for ~3.5 h. In SK-1 strains of *S. cerevisiae* the total duration of the prophase stages showing SC materials last for ~2.3 h (Padmore et al., 1991). As in *S. cerevisiae*, we observed an interval of more than 1 h between completion of DNA replication and the appearance of the first short elements (Fig. 3 *c*). The elements are dissolved shortly before the first meiotic division. The time course experiments reveal different prophase stages that are defined by the morphology of the elements (Fig. 3). The different classes of spread nuclei (Fig. 1) thus correspond to successive stages of prophase I. Nuclei of class I (short segments of elements, Fig. 1, *b* and *h*) make an exception because they represent the earliest as well as the latest cytologically detectable prophase stage (Fig. 3, *a* and *d*). Morphologically, these two
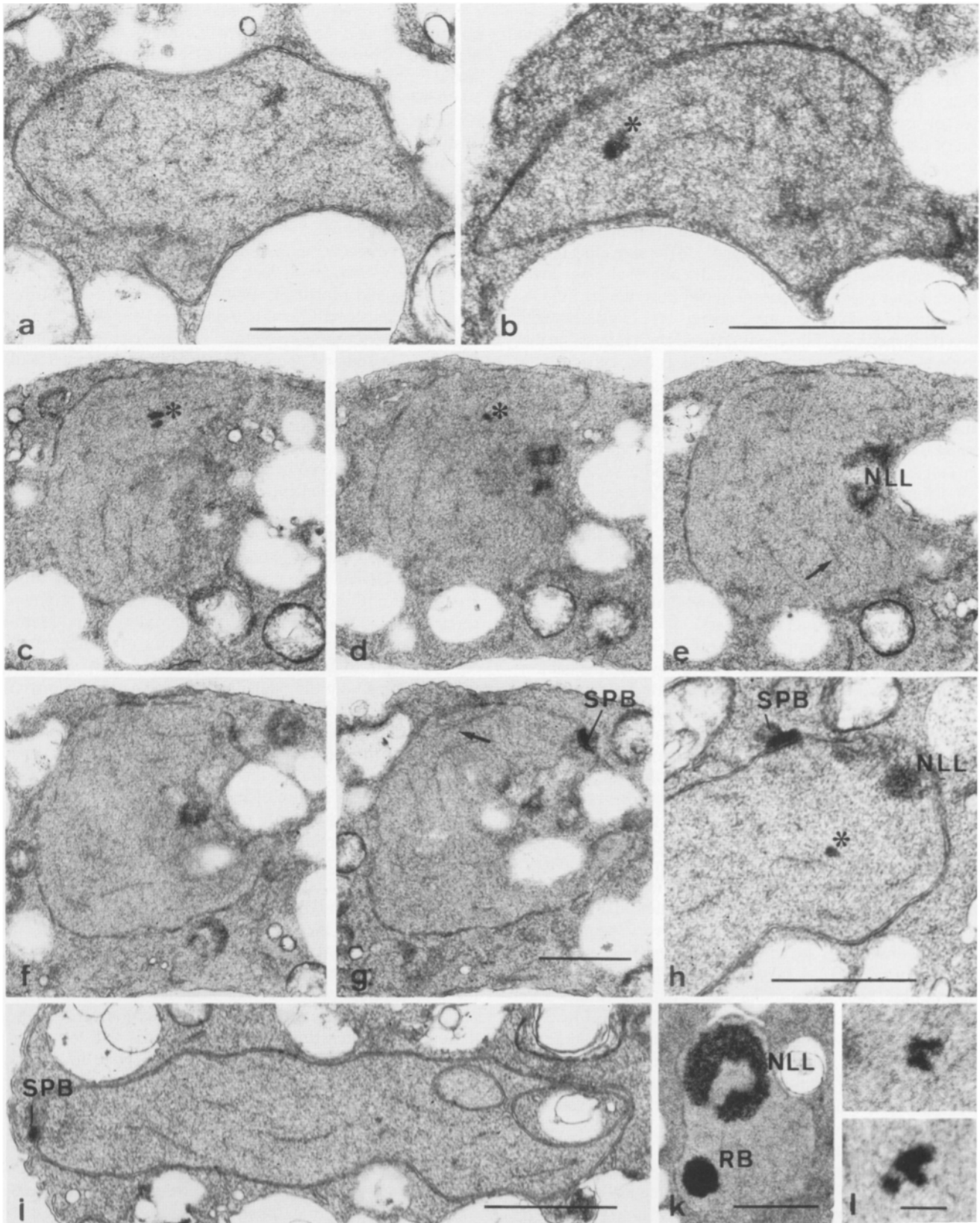
Figure 7. Electron micrographs of sections from meiotic nuclei. (*Asterisk*) "black bodies" (possibly corresponding to centromeres); (*NLL*) nucleolus. (*a* and *b*) Nuclei with deformed shapes and linear elements running in random directions overall. Some elements seem to be interconnected (early prophase). (*c–g*) Series of sections 5 to 7 and 9, 10 of the same nucleus. The nucleus is strongly bent and the elements mainly follow the direction of the nuclear membrane. *Arrows* (*e* and *g*): parallel "alignment" of two elements. (*h*) Typical arrangement showing the SPB lying on the nuclear membrane close to the nucleolus and the "black bodies" facing the SPB (the same arrangement is obvious in different sections in *c–g*). (*i*) Strongly elongated nucleus with single linear elements running mainly in longitudinal directions. The SPB lies at the left end of the nucleus (late prophase). (*k*) Nucleus revealing a prominent "round body" (*RB*) near the nucleolus. (*l*) Two consecutive sections showing the "black bodies" at higher magnification. Bars, 1 μm (*a–k*), 200 nm (*l*).

stages could not be distinguished. The short elements of stage 1 grow and turn into networks (class IIa; Fig. 1, c and d) and bundles of elements (class IIb; Fig. 1, e and f). Nuclei of class IIa and b can not be separated temporally, but those of class IIb are much rarer (Fig. 3 a and d). They might either correspond to a distinct stage or to a different manifestation of the same stage. We designate both class IIa and IIb nuclei as belonging to stage 2. There are several lines of evidence which argue against the possibility that nuclei of stage 2 represent artifacts of spreading. (a) They show a dynamic appearance and disappearance during early prophase as it is expected for a true stage. (b) Changes in the spreading conditions (see Materials and Methods) did not result in changes of the relative portion of class II nuclei (not shown). (c) Observations in serially sectioned nuclei were consistent with class II morphology (Fig. 7, a–g). However, it is possible that the elements become more entangled as a consequence of the spreading process. The networks might therefore reflect that the elements (and the chromosomes) occupy more or less random positions in the nucleus during stage 2 (see below). Before the elements are degraded again, they appear as long and single elements in spreads (Fig. 1 g) and in sections (Fig. 7 i) defining prophase stage 3. Nuclei with single elements are often more spread out than those of class II (e.g., compare Fig. 1, d with g). It seems that the chromatin is held together more strongly if the elements are connected. This is another indication that the chromatin is anchored to the elements, besides the occasional association of "chromatin loops" with the elements (Fig. 2 a).

Meiosis following mating of haploid cells is less synchronous than azygotic meiosis. However, since the haplontic S. pombe cells normally undergo zygotic meiosis we also checked prophase nuclei in zygotes. During zygotic meiosis we observed the same temporal order of prophase stages confirming our results obtained in azygotic meiosis. Moreover, the elements are meiosis-specific since they were not observed in heterothallic strains shifted to meiotic conditions.

The meiotic prophase stages and their sequence could be confirmed by time course experiments with a diploid strain homozygous for mei4-B2. This mutation probably plays a regulatory role during meiotic prophase (see Introduction). Mutants are arrested after DNA replication and before the first meiotic division (Fig. 3 e). During early prophase the timing of the events in wild-type and mei4-B2 meiosis is similar (compare Fig. 3, a–c with Fig. 3, d and e). Later during prophase, nuclei containing single elements (stages 3 and 4) become highly enriched in the mei4-B2 strain (Fig. 3 d). We cannot decide whether the block is mainly at stage 3 with subsequent unspecific degradation of the elements in the arrested nuclei or whether stage 4 is the main stage where the cells are blocked. In the latter case there would be some delay during prophase reflected by the high proportions of stages 2 and 3 at late times. Alternatively, the block in stage 3 is not tight. However, there are no cells performing the first meiotic division (Fig. 3 e) and no duplicated SPBs have been observed (not shown). Possibly the point of arrest of mei4-B2 mutants defines a cell-cycle checkpoint (Hartwell and Weinert, 1989). These checkpoints seem to exist also in meiosis and an important arrest point is at the end of pachytene in other organisms (e.g., Maller, 1985; Shuster and Byers, 1989, and references cited therein). Alternatively, mei4-B2 strains are lacking one or several gene functions that are directly required for the transition out of prophase.

We have counted and measured the linear elements in haploid, diploid, and tetraploid mei4-B2 strains. Six linear elements would be expected in a diploid nucleus if each element would represent a continuous axial core. However, the nuclei contain more than the expected number of elements (Table II). Thus, the elements are apparently not formed continuously over the whole length of each chromosome (Fig. 8 a). In other organisms fragments of axial elements that do not cover the whole chromosome are found before SC formation (von Wettstein et al., 1984). The total element length in a diploid strain (34 μm) is smaller than the total length of synapsed axial elements in S. cerevisiae ($\sim$58 μm; e.g., Loidl et al., 1991). Both yeasts have about the same genome size (e.g., King and Mortimer, 1990). Thus, provided that the linear elements correspond to axial cores, the chromatin of S. pombe is packed more densely into the elements than in S. cerevisiae and/or S. pombe has considerable stretches of chromatin that is not packed into elements. The continuous variation in element length (see Results and Fig. 6) argues against a fixed formation of the elements at always the same regions of the chromosomes. However, such a constant formation might be obscured by a rapid and asynchronous degradation of the linear elements during late prophase. For several reasons it is unlikely that there is considerable fragmentation of the elements during spreading. (a) In nuclei which were strongly spread out (large diameter), we did not find more or smaller elements on average than in nuclei which were less spread out (data not shown). (b) If weaker or stronger spreading conditions were applied (see Materials and Methods), there was no change in the distribution of element number and length (data not shown). (c) The 18 to 30 elements found in spread diploid nuclei are in good accordance with our results from serial sections, and with the 25 to 30 elements observed by Olson et al. (1978). (d) Finally, our spreading method is gentle and the axial cores of other eukaryotes are rarely broken during this process (observations of J. Loidl). The mean sum of element lengths per nucleus correlates well with the ploidy of the strains whereas there is no such direct correlation with the number of elements per nucleus. The haploid nuclei contain relatively more and the tetraploid nuclei relatively fewer elements compared to the diploid nuclei (Table II). This observation might reveal intrinsic differences in the prophase chromatin organization of strains with different ploidy. However, it was difficult to consider equivalent sets of nuclei in the different strains because the haploid strain was delayed in prophase whereas the tetraploid strain showed a precipitated prophase compared to the diploid strain. It is noteworthy that haploid and tetraploid strains show the same classes of spread nuclei like the diploid strain (Fig. 5).

We never observed, neither in spread nor in sectioned nuclei, any indication of a regular pairing of the linear elements into a tripartite SC. The same nuclear structures were detected with two independent methods that reliably reveal SCs in other organisms (Fig. 2 b). It seems that no central elements are formed in S. pombe. Because it is possible to check hundreds of spread nuclei in a short time, and considering the incomplete synchrony of our meiotic cells, we certainly would have detected SCs even if they were formed for only a small period of prophase I. Because the classical meiotic prophase stages are defined by the morphogenesis of the SC we can not assign these stages in fission yeast. There are indications that the whole genus Schizosaccharomyces does
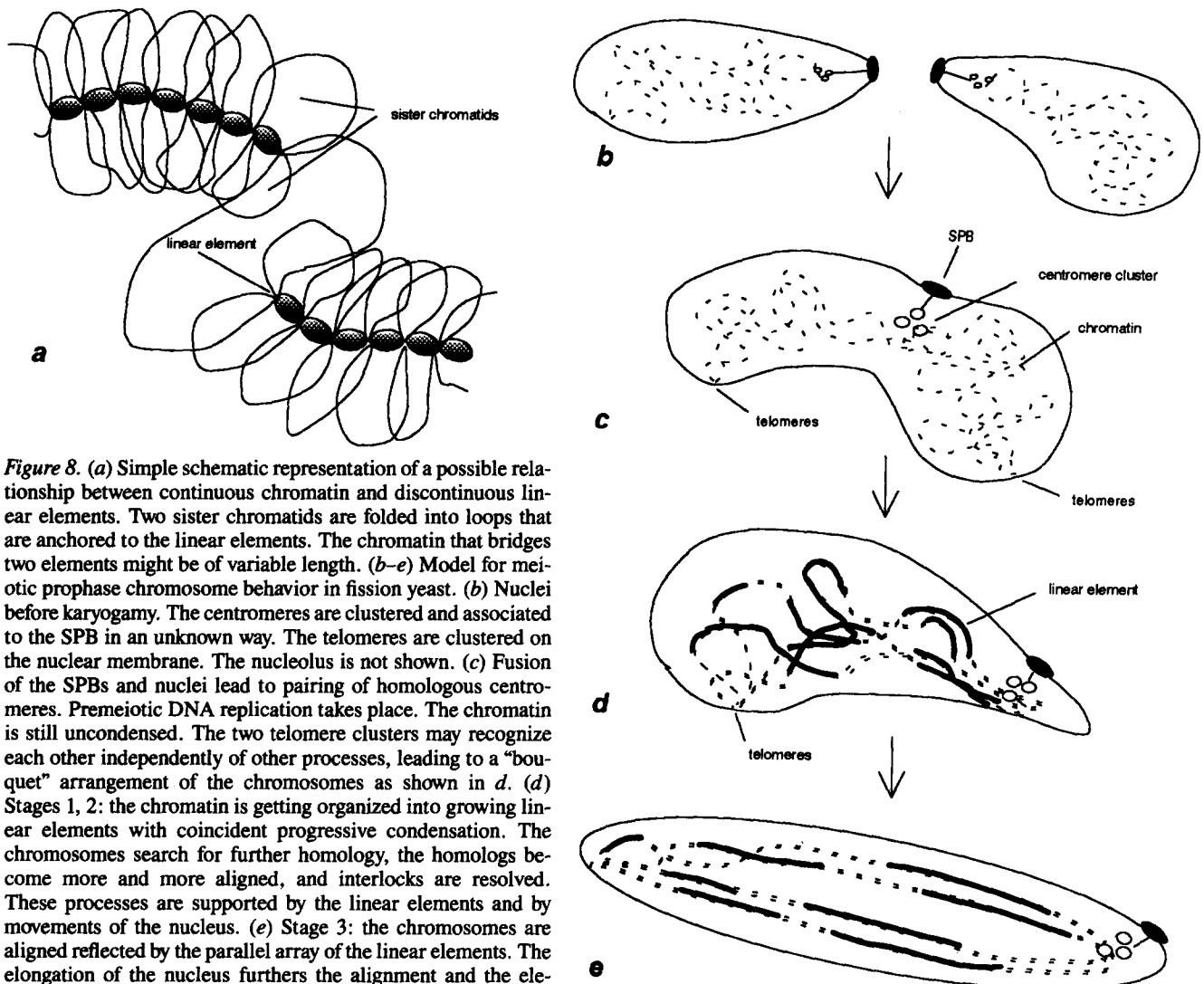
Figure 8. (a) Simple schematic representation of a possible relationship between continuous chromatin and discontinuous linear elements. Two sister chromatids are folded into loops that are anchored to the linear elements. The chromatin that bridges two elements might be of variable length. (b-e) Model for meiotic prophase chromosome behavior in fission yeast. (b) Nuclei before karyogamy. The centromeres are clustered and associated to the SPB in an unknown way. The telomeres are clustered on the nuclear membrane. The nucleolus is not shown. (c) Fusion of the SPBs and nuclei lead to pairing of homologous centromeres. Premeiotic DNA replication takes place. The chromatin is still uncondensed. The two telomere clusters may recognize each other independently of other processes, leading to a "bouquet" arrangement of the chromosomes as shown in d. (d) Stages 1, 2: the chromatin is getting organized into growing linear elements with coincident progressive condensation. The chromosomes search for further homology, the homologs become more and more aligned, and interlocks are resolved. These processes are supported by the linear elements and by movements of the nucleus. (e) Stage 3: the chromosomes are aligned reflected by the parallel array of the linear elements. The elongation of the nucleus furthers the alignment and the elements provide structural support for the order. After establishment of functional chiasmata the linear elements are dissolved and the SPB separates in preparation for the first meiotic division.

not form SCs. In *S. japonicus* var. *japonicus*, Tanaka and Hirata (1982) observed the same nuclear prophase structures as in *S. pombe*. Spread nuclei of *S. japonicus* var. *versatilis* revealed identical classes of linear elements as described here for *S. pombe* (J. Bähler and A. Svoboda, unpublished observation). Ashton and Moens (1982) failed to detect SCs in *S. octosporus*, and we have indications from spread nuclei that also this species forms linear elements.

We also analyzed DAPI-stained standard and *mei4-B2* cells in the time course experiments (Fig. 3, *b* and *e*). Three types of meiotic prophase nuclei were distinguished according to the shape and staining behavior of their chromatin region (Fig. 4). Some nuclei were difficult to classify unambiguously however, because they showed an intermediate stage. Besides this, the shape of the chromatin region might be different, depending on the angle of observation. In particular the number of deformed nuclei might be underestimated because they are not discovered at every angle. Nevertheless, we think that the classification of DAPI-stained nuclei reveals some interesting aspects. Early during prophase the

chromatin seems to undergo dramatic changes of shape (deformed nuclei), before it is maximally stretched out for a short time (horse tail nuclei). During the major part of meiotic prophase the nuclei are elongated. We observed the highly elongated horse tail nuclei more frequently in prophase of a zygotic meiosis where they appear after the fusion of two teardrop-shaped nuclei (data not shown, see also Ashton and Moens, 1982). The nuclei seem to move in the cell during prophase as can be concluded from our observations and from observations with *S. japonicus* var. *versatilis* (A. Svoboda, personal communication). The deformed nuclei coincide reasonably well with stage 2, whereas the horse tail and most elongated nuclei correspond to stage 3 (Fig. 3, *a-c*). This is further corroborated by the experiment with the *mei4-B2* cells where nuclei with single elements and elongated shape become highly enriched (Fig. 3, *d* and *e*). These correlations fit well with the observations made in serial sections. The sectioned nuclei being most indicative of stage 2 morphology often showed strikingly deformed shapes (Fig. 7, *a-g*). Sectioned nuclei with single and ordered linear ele-

ments on the other hand were mostly elongated (Fig. 7 *i*). The longitudinally arranged elements in these nuclei appear randomly distributed after spreading, possibly because the nuclei become spherical before spreading.

By DAPI-staining of spread or squashed meiotic prophase nuclei we never detected a strong chromosome condensation before metaphase I (unpublished observations). However, the chromosomes of *S. pombe* reveal some degree of condensation during prophase I in DAPI-stained whole cells. Especially in the horse tail nuclei a filamentous appearance of the chromatin is apparent. Generally, the staining is more intense in prophase nuclei. During metaphase and anaphase highly condensed chromosomes are visible and sometimes three separate units can be resolved (Robinow, 1977; our observations). Thus, *S. pombe* seems to behave similar to other eukaryotes with regard to chromosome condensation.

In contrast to *S. cerevisiae* (reviewed by Byers, 1981) the SPB of *S. pombe* is not duplicated during meiotic prophase (Hirata and Tanaka, 1982; our observations). Duplication of the SPB seems to occur shortly after degradation of the elements. We never observed any fragments of elements in nuclei with duplicated SPBs. During prophase I the SPB appears as a tripartite body in spread nuclei, possibly reflecting discs or satellites of the SPB in a doubling stage (Fig. 1). We rarely detected small bodies lying on the SPB also in sections (not shown). In spreads and in sections the SPB is found adjacent to the nucleolus during prophase I (Fig. 1, *b–h* and Fig. 7, *c–h*), but not so in other stages (Fig. 1, *a* and *i*). In each serially sectioned nucleus we observed a cluster of electron-dense bodies which we designated as "black bodies" (Fig. 7, *b–d*, *h*, *l*). The black bodies seem to consist of three single bodies of different size. We propose that the black bodies represent the centromeres. In fungi it is usual that the centromere is the only chromatin region that can be detected in sections (e.g., Carmi et al., 1978; Holm et al., 1981; Leblon et al., 1986; Bojko, 1988). The nucleolus, the black bodies, and the SPB seem to maintain their spatial arrangement throughout prophase with the black bodies lying opposite to the SPB (Fig. 7 *h*).

Significance of the Nuclear Structures for Meiosis

How does *S. pombe* succeed to pair, recombine, and segregate the homologous chromosomes during meiosis I without developing a classical SC? What is the nature of the linear elements and what role do they play in fission yeast meiosis? Because the SC is a remarkably conserved structure in the great majority of eukaryotes, it seems to be an early invention of meiosis (Maguire, 1992). It is unlikely that fission yeasts separated from a common ancestor before the SC had evolved. Therefore, the linear elements are probably derived from SC components and are likely to correspond to the axial cores (see above). They might represent evolutionary relics without function. However, it is expensive for a species to maintain such prominent structures like the linear elements and the dynamic behavior of the elements, defining different prophase stages, suggests that they play some role. Abnormal organization of the linear elements in meiotic mutants would also argue for a function. We have indications that the elements are shorter and less abundant in cells containing the regulatory mutation *patl-114*. The abnormalities

may be related to the reduced meiotic recombination frequencies in *patl-114* cells (Iino and Yamamoto, 1985; Bähler et al., 1991). In the following, we propose a model that correlates the arrangement of cytological structures with chromosome behavior during prophase I of fission yeast. We try to point out a mechanism for chromosome pairing and suggest possible tasks of the linear elements during meiotic prophase.

Recently it was shown that the centromeres are clustered near the SPB in vegetative cells of *S. pombe* (Uzawa and Yanagida, 1992; Takahashi et al., 1992). In situ hybridizations on spread meiotic nuclei reveal a centromere and a telomere cluster in different regions of the nucleus. The clusters generally consist of three bodies (H. Scherthan and J. Bähler, unpublished results). Genetic data show that mitotic chromosome pairing in diploid cells of *S. pombe* is usually restricted to the centromere region (Minet et al., 1980). In sections, we detected the presumptive centromeres facing the SPB (see above). It is known that karyogamy is preceded by fusion of the SPBs (Hirata and Tanaka, 1982; Ashton and Moens, 1982). We propose that the clustered centromeres and the SPB are connected throughout the life cycle of fission yeast. The fusion of the two SPBs after mating, followed by karyogamy, brings the centromeres of the two chromosome sets together. Within the resulting cluster the homologous centromeres recognize each other, providing a rapid initiation of chromosome pairing, a special requirement for a haplontic organism (Fig. 8, *b* and *c*). In many organisms the chromosomes occupy a polarized centromere-telomere arrangement in the nucleus (Fussell, 1987; Hiraoka et al., 1990) which is also suggested by our in situ hybridization data (see above). Such a defined spatial order of the chromatin might minimize movements of chromosomes during pairing. We further suggest that subsequent to the initial recognition events at the centromeres, the formation of the linear elements is initiated at different sites on each chromosome, facilitating alignment of the chromosomes from centromere to telomeres (Fig. 8, *c* and *d*). This might be achieved simply by an architectural role of the elements in supporting the condensation of chromatin (see also Smithies and Powers, 1986). Additionally, the elements might bring corresponding DNA segments on homologous chromosomes into register by lining up the chromatin, hence, presenting an ordered subset of sequences to the homologous partner. Thus, the organization of the chromatin in the linear elements might directly facilitate the search for homology which possibly corresponds to the initiation of recombination (Kleckner et al., 1991, and references cited therein). Furthermore, the linear elements might function in the recognition and resolution of chromosomal tangles (interlocks). Interlocks are potentially generated by the progressive alignment of randomly positioned chromosomes, and it has been suggested that SC formation is involved in their resolution (Rasmussen, 1986; Kleckner et al., 1991). The nuclei are often deformed at prophase stages 1 and 2, possibly due to movements that support the processes of chromosome alignment. The prominent elongation of the nucleus during stage 3 might keep the homologous chromosomes aligned longitudinally with help of the elements (Fig. 8 *e*). The alignment of bivalents might lead to proximity of chromosome regions that were not involved in primary homolog recognition, yielding additional

opportunities for recombination events. In *S. pombe*, the whole process never culminates in a close synapsis of the linear elements into a continuous SC.

Further work is needed for the correlation of recombination events (initiation, resolution) with cytological stages. Likewise, it remains to be investigated whether the parallel arrays of linear elements in sections correspond to the alignment of homologous chromosomes over long stretches. Contacts between the chromosomes at the DNA level are expected at the centromeres and telomeres (see above) and at the numerous sites of recombination. Preliminary data on mutants deficient in meiotic recombination indicate that recombination is required for proper reductional chromosome segregation in *S. pombe* (see Introduction). The elements might also function in the establishment of functional chiasmata or sister chromatid cohesiveness to prevent a premature separation of homologous chromosomes. This function has been attributed to the SC in other organisms (e.g., Maguire, 1978, 1990; Engebrecht et al., 1990).

Why do most eukaryotes develop a tripartite SC, but not *S. pombe*? There are now many pieces of evidence that pairing of homologous chromosomes and recombination can occur without SC formation. The observations of a presynaptic alignment of the homologous chromosomes before pachytene shows that the recognition of homologous chromosomes occurs early in prophase (Loidl, 1990; Scherthan et al., 1992). At least a portion of the crossover events can occur in the absence of a complete SC, and crossing-over may be responsible for the development of the SC rather than vice versa (reviewed by Roeder, 1990). Double-strand breaks which are thought to be involved in the initiation of meiotic recombination are detected prior to synapsis (Padmore et al., 1991). We think that there is a correlation between the absence of a SC and the absence of crossover interference in *S. pombe* (see Introduction). This correlation is attractive because a transfer of information along a bivalent is required for interference. Apparently such an information transfer leading to suppression of neighboring exchange events, may be accomplished by a continuous SC or during its formation (e.g., by the developing central element). However, the SC is probably a multifunctional structure with other tasks besides regulation of crossover distribution. Especially in higher eukaryotes it might also be required for the managing and regular pairing of the many large chromosomes that contain widespread repetitive sequences.

Conclusions and Future Questions

S. pombe is highly proficient for meiotic recombination and manages to segregate its homologous chromosomes during meiosis I without developing a classical tripartite SC. The linear elements that appear during meiotic prophase reveal different stages that are also characterized by striking changes in the shape of the nucleus. These elements are not formed continuously along the chromosomes and they most likely correspond to fragments of axial elements. We propose a model that provides an efficient process for the recognition of homologous chromosomes at the centromeres and assigns functions to the linear elements in the preparation of the chromosomes for faithful segregation during the first meiotic division. Possibly *S. pombe* needs no SC because it can afford

a random distribution of crossover events along its bivalents. Mutations in other organisms should give further insight into the relation between SC formation and crossover interference. The linear elements, together with other special features of fission yeast, may define those structures that are truly required for chromosome pairing, meiotic recombination, and segregation of homologous chromosomes. The study of fission yeast meiosis is promising for a better understanding of the events occurring during meiotic prophase and of the role that the SC plays in other organisms.

With the establishment of the spreading technique, fission yeast becomes amenable to combined genetic, molecular, and cytological approaches. If the linear elements really do have a function in meiosis they should be altered in some mutants, and useful to characterize the many known meiotic recombination mutations (Ponticelli and Smith, 1989; DeVeaux et al., 1992). It will be interesting to correlate the timing of recombination events detected by physical assays with the prophase stages defined by the linear elements. The spread nuclei are suitable for in situ hybridization (Scherthan et al., 1992; our observations) as well as for immunocytology (Dresser, 1987; Klein et al., 1992; our observations). These two techniques will be fruitful for the study of the structure and function of meiotic chromosomes and their pairing behavior. It is of great interest to know whether in *S. pombe* structural proteins of the SC are preserved, and which proteins are missing. This will contribute to define the roles of various SC proteins.

References

Ashton, M.-L., and P. B. Moens. 1982. Light and electron microscopy of conjugation in the yeast, *Schizosaccharomyces octosporus*. *Can. J. Microbiol.* 28:1059–1077.

Bähler, J., P. Schuchert, C. Grimm, and J. Kohli. 1991. Synchronized meiosis and recombination in fission yeast: observations with *pat1-114* diploid cells. *Curr. Genet.* 19:445–451.

Baker, B. S., A. T. C. Carpenter, M. S. Esposito, R. E. Esposito, and L. Sandler. 1976. The genetic control of meiosis. *Annu. Rev. Genet.* 10:53–134.

Beach, D., L. Rodgers, and J. Gould. 1985. *RAN1+* controls the transition from mitotic division to meiosis in fission yeast. *Curr. Genet.* 10:297–311.

Bojko, M. 1988. Presence of abnormal synaptonemal complexes in heterothallic species of *Neurospora*. *Genome*. 30:697–709.

Bresch, C., G. Müller, and R. Egel. 1968. Genes involved in meiosis and sporulation of a yeast. *Mol. Gen. Genet.* 102:301–306.

Byers, B. 1981. Cytology of the yeast life cycle. *In* The Molecular Biology of the Yeast *Saccharomyces*: Life Cycle and Inheritance. J. Strathern, E. W. Jones, and J. Broach, editors. Cold Spring Harbor Laboratory, Cold Spring Harbor, New York. 59–85.

Carmi, P., P. B. Holm, Y. Koltin, S. W. Rasmussen, J. Sage, and D. Zickler. 1978. The pachytene karyotype of *Schizophyllum commune* analyzed by three dimensional reconstruction of synaptonemal complexes. *Carlsberg Res. Commun.* 43:117–132.

Carpenter, A. T. C. 1988. Thoughts on recombination nodules, meiotic recom-

bination, and chiasmata. *In* Genetic Recombination. R. Kucherlapati, and G. R. Smith, editors. American Society for Microbiology, Washington, D.C. 497–527.

Clutterbuck, A. J. 1992. Sexual and parasexual genetics of *Aspergillus* species. *In Aspergillus*: Biology and Industrial Applications. J. W. Bennett, M. A. Klich, editors. Butterworth-Heinemann, Boston. 3–18.

DeVeaux, L. C., N. A. Hoagland, and G. R. Smith. 1992. Seventeen complementation groups of mutations decreasing meiotic recombination in *Schizosaccharomyces pombe. Genetics*. 130:251–262.

Dresser, M. E. 1987. The synaptonemal complex and meiosis: an immunocytochemical approach. *In* Meiosis. P. B. Moens, editor. Academic Press, New York. 245–274.

Dresser, M. E., and C. N. Giroux. 1988. Meiotic chromosome behavior in spread preparations of yeast. *J. Cell Biol.* 106:567–573.

Egel, R. 1973. Commitment to meiosis in fission yeast. *Mol. Gen. Genet.* 121:277–284.

Egel, R. 1978. Synaptonemal complex and crossing-over: structural support or interference? *Heredity.* 41:233–237.

Egel, R., and M. Egel-Mitani. 1974. Premeiotic DNA synthesis in fission yeast. *Exp. Cell Res.* 88:127–134.

Egel-Mitani, M., L. W. Olsen, and R. Egel. 1982. Meiosis in *Aspergillus nidulans*: another example for lacking synaptonemal complexes in the absence of crossover interference. *Hereditas.* 97:179–187.

Engebrecht, J. A., J. Hirsch, G. S. Roeder. 1990. Meiotic gene conversion and crossing over: their relationship to each other and to chromosome synapsis and segregation. *Cell.* 62:927–937.

Fahrenbach, W. H. 1984. Continuous serial thin sectioning for electron microscopy. *J. Electron Microsc. Tech.* 1:387–398.

Fussell, C. P. 1987. The Rabl orientation: a prelude to synapsis. *In* Meiosis. P. B. Moens, editor. Academic Press, New York. 275–299.

Giroux, C. N. 1988. Chromosome synapsis and meiotic recombination. *In* Genetic Recombination. R. Kucherlapati, and G. R. Smith, editors. American Society for Microbiology, Washington, D.C. 465–496.

Giroux, C. N., M. E. Dresser, and H. F. Tiano. 1989. Genetic control of chromosome synapsis in yeast meiosis. *Genome.* 31:81–87.

Gutz, H. 1963. Untersuchungen zur Feinstruktur der Gene *ade7* und *ade6* von *Schizosaccharomyces pombe* LIND. Habilitationsschrift, Berlin. 68–74.

Gutz, H., H. Heslot, U. Leupold, and N. Loprieno. 1974. *Schizosaccharomyces pombe. In* Handbook of Genetics, Vol. 1. R. C. King, editor. Plenum Publishing Corp., New York. 395–446.

Hartwell, L. H., and T. A. Weinert. 1989. Checkpoints: controls that ensure the order of cell cycle events. *Science (Wash. DC).* 246:629–634.

Hiraoka, Y., D. A. Agard, and J. W. Sedat. 1990. Temporal and spatial coordination of chromosome movement, spindle formation, and nuclear envelope breakdown during prometaphase in *Drosophila melanogaster* embryos. *J. Cell Biol.* 111:2815–2828.

Hirata, A., and K. Tanaka. 1982. Nuclear behavior during conjugation and meiosis in the fission yeast *Schizosaccharomyces pombe. J. Gen. Appl. Microbiol.* 28:263–274.

Holm, P. B., S. W. Rasmussen, D. Zickler, B. C. Lu, and J. Sage. 1981. Chromosome pairing, recombination nodules and chiasma formation in the basidiomycete *Coprinus cinereus. Carlsberg Res. Commun.* 46:305–346.

Iino, Y., and M. Yamamoto. 1985. Negative control for the initiation of meiosis in *Schizosaccharomyces pombe. Proc. Natl. Acad. Sci. USA.* 82:2447–2451.

Jones, G. H. 1987. Chiasmata. *In* Meiosis. P. B. Moens, editor. Academic Press, New York. 213–238.

Käfer, E. 1977. Meiotic and mitotic recombination in *Aspergillus* and its chromosomal aberrations. *Adv. Genet.* 19:33–131.

King, J. S., and R. K. Mortimer. 1990. A polymerization model of chiasma interference and corresponding computer simulation. *Genetics.* 126:1127–1138.

Kleckner, N., R. Padmore, and D. K. Bishop. 1991. Meiotic chromosome metabolism: one view. *Cold Spring Harbor Symp. Quant. Biol.* 56:729–743.

Klein, F., T. Laroche, M. E. Cardenas, J. F.-X. Hofmann, D. Schweizer, and S. M. Gasser. 1992. Localization of RAP1 and Topoisomerase II in nuclei and meiotic chromosomes of yeast. *J. Cell Biol.* 117:935–948.

Kohli, J., H. Hottinger, P. Munz, A. Strauss, and P. Thuriaux. 1977. Genetic mapping in *Schizosaccharomyces pombe* by mitotic and meiotic analysis and induced haploidization. *Genetics.* 87:471–489.

Leblon, G., D. Zickler, and S. Lebilcot. 1986. Most UV-induced reciprocal translocations in *Sordaria macrospora* occur in or near centromere regions. *Genetics.* 112:183–204.

Loidl, J. 1990. The initiation of meiotic chromosome pairing: the cytological view. *Genome.* 33:759–778.

Loidl, J. 1991. Coming to grips with a complex matter. A multidisciplinary approach to the synaptonemal complex. *Chromosoma.* 100:289–292.

Loidl, J., K. Nairz, and F. Klein. 1991. Meiotic chromosome synapsis in a haploid yeast. *Chromosoma.* 100:221–228.

Maguire, M. P. 1978. A possible role for the synaptonemal complex in chiasma maintenance. *Exp. Cell Res.* 112:297–308.

Maguire, M. P. 1990. Sister chromatid cohesiveness: vital function, obscure mechanism. *Biochem. Cell Biol.* 68:1231–1242.

Maguire, M. P. 1992. The evolution of meiosis. *J. Theor. Biol.* 154:43–55.

Maller, J. 1985. Regulation of oocyte maturation. *Cell Differ.* 16:211–221.

Minet, M., A. M. Grossenbacher-Grunder, and P. Thuriaux. 1980. The origin of a centromere effect on mitotic recombination. *Curr. Genet.* 2:53–60.

Moses, M. 1968. Synaptinemal complex. *Annu. Rev. Genet.* 2:363–412.

Munz, P., K. Wolf, J. Kohli, and U. Leupold. 1989. Genetics overview. *In* Molecular Biology of the Fission Yeast. A. Nasim, P. Young, and B. F. Johnson, editors. Academic Press, San Diego, California. 1–30.

Olson, L. W., U. Edén, M. Egel-Mitani, and R. Egel. 1978. Asynaptic meiosis in fission yeast? *Hereditas.* 89:189–199.

Padmore, R., L. Cao, and N. Kleckner. 1991. Temporal comparison of recombination and synaptonemal complex formation during meiosis in *S. cerevisiae. Cell.* 66:1239–1256.

Ponticelli, A. S., and G. R. Smith. 1989. Meiotic recombination-deficient mutants of *Schizosaccharomyces pombe. Genetics.* 123:45–54.

Rasmussen, S. W. 1986. Initiation of synapsis and interlocking of chromosomes during zygotene in *Bombyx* spermatocytes. *Carlsberg Res. Commun.* 51:401–432.

Rattner, J. B., M. Goldsmith, and B. A. Hamkalo. 1980. Chromatin organization during meiotic prophase of *Bombyx mori. Chromosoma.* 79:215–224.

Rattner, J. B., M. R. Goldsmith, and B. A. Hamkalo. 1981. Chromosome organization during male meiosis in *Bombyx mori. Chromosoma.* 82:341–351.

Reynolds, E. S. 1963. The use of lead citrate at high pH as electron-opaque stain in electron microscopy. *J. Cell Biol.* 17:208–212.

Robinow, C. F. 1977. The number of chromosomes in *Schizosaccharomyces pombe*: light microscopy of stained preparations. *Genetics.* 87:491–497.

Robinow, C. F., and J. S. Hyams. 1989. General cytology of fission yeast. *In* Molecular Biology of the Fission Yeast. A. Nasim, P. Young, and B. F. Johnson, editors. Academic Press, San Diego, California. 273–330.

Roeder, G. S. 1990. Chromosome synapsis and genetic recombination: their roles in meiotic chromosome segregation. *Trends Genet.* 6:385–389.

Rowley III, J. C., and D. T. Moran. 1975. A simple procedure for mounting wrinkle-free sections on formvar-coated slot grids. *Ultramicroscopy.* 1:151–155.

Scherthan, H., J. Loidl, T. Schuster, and D. Schweizer. 1992. Meiotic chromosome condensation and pairing in *S. cerevisiae* studied by chromosome painting. *Chromosoma.* 101:590–595.

Shimoda, C., A. Hirata, M. Kishida, T. Hashida, and K. Tanaka. 1985. Characterization of meiosis-deficient mutants by electron microscopy and mapping of four essential genes in the fission yeast *Schizosaccharomyces pombe. Mol. Gen. Genet.* 200:252–257.

Shuster, E. O., and B. Byers. 1989. Pachytene arrest and other meiotic effects of the start mutations in *Saccharomyces cerevisiae. Genetics.* 123:29–43.

Smithies, O., and P. Powers. 1986. Gene conversions and their relationship to homologous chromosome pairing. *Phil. Trans. R. Soc. Lond. B. Biol. Sci.* 312:291–302.

Snow, R. 1979. Maximum likelihood estimation of linkage and interference from tetrad data. *Genetics.* 92:231–245.

Strickland, W. N. 1958. An analysis of interference in *Aspergillus nidulans. Proc. R. Soc. Lond. B. Biol. Sci.* 149:82–101.

Szankasi, P., and G. R. Smith. 1992. A DNA exonuclease induced during meiosis of *Schizosaccharomyces pombe. J. Biol. Chem.* 267:3014–3023.

Takahashi, K., S. Murakami, Y. Chikashige, H. Funabiki, O. Niwa, and M. Yanagida. 1992. A low copy number central sequence with strict symmetry and unusual chromatin structure in fission yeast centromere. *Mol. Biol. Cell.* 3:819–835.

Tanaka, K., and A. Hirata. 1982. Ascospore development in the fission yeasts *Schizosaccharomyces pombe* and *S. japonicus. J. Cell Sci.* 56:263–279.

Toda, T., M. Yamamoto, and M. Yanagida. 1981. Sequential alterations in the nuclear chromatin region during mitosis of the fission yeast *Schizosaccharomyces pombe*: video fluorescence microscopy of synchronously growing wild-type and cold-sensitive *cdc* mutants by using a DNA-binding fluorescence probe. *J. Cell Sci.* 52:271–287.

Uzawa, S., and M. Yanagida. 1992. Visualization of centromeric and nucleolar DNA in fission yeast by fluorescence in situ hybridization. *J. Cell Sci.* 101:267–275.

von Wettstein, D., S. W. Rasmussen, and P. B. Holm. 1984. The synaptonemal complex in genetic segregation. *Annu. Rev. Genet.* 18:331–413.

Watanabe, Y., Y. Iino, K. Furuhata, C. Shimoda, and M. Yamamoto. 1988. The *S. pombe mei2* gene encoding a crucial molecule for commitment to meiosis is under the regulation of cAMP. *EMBO (Eur. Mol. Biol. Organ.) J.* 7:761–767.

Weith, A. 1985. The fine structure of euchromatin and centromeric heterochromatin in *Tenebrio molitor* chromosomes. *Chromosoma.* 91:287–296.